

Modified Layered Double Hydroxide Mg/M³⁺ (M³⁺ = Al and Cr) Using Metal Oxide (Cu) as Adsorbent for Methyl Orange and Methyl Red Dyes

Alfan Wijaya¹, Patimah Mega Syah Bahar Nur Siregar¹, Arini Fousty Badri², Neza Rahayu Palapa², Amri Amri¹, Nur Ahmad¹, Aldes Lesbani^{1,2*}

¹ Research Center of Inorganic Materials and Complexes, Faculty of Mathematics and Natural Sciences, Sriwijaya University, Jl. Padang Selasa, Bukit Besar, Palembang 30139, South Sumatra, Indonesia

² Graduate School, Faculty of Mathematics and Natural Sciences, Sriwijaya University, Jl. Padang Selasa, Bukit Besar, Palembang 30139, South Sumatra, Indonesia

* Corresponding author, e-mail: aldeslesbani@pps.unsri.ac.id

Received: 28 November 2022, Accepted: 16 February 2023, Published online: 27 March 2023

Abstract

Mg/Cr-layered double hydroxide (Mg/Cr-LDH) and Mg/Al-layered double hydroxide (Mg/Al-LDH) intercalated metal oxide (Mg/Cr-Cu and Mg/Al-Cu) were synthesized by the co-precipitation method which is indicated by the X-ray diffraction (XRD), Fourier-transform infrared spectroscopy (FTIR), and Brunauer Emmett Teller (BET) analysis. Mg/Cr-LDH intercalated metal oxide increased its surface area from 21.5 to 38.9 m²/g, while the surface area of Mg/Al-LDH from 23.2 to 30.5 m²/g. The adsorption capacity of Mg/Cr-Cu is 64.156 mg/g for methyl orange (MO) and 78.740 mg/g for methyl red (MR), and the adsorption capacity of Mg/Al-Cu is 97.087 mg/g for MO and 108.696 mg/g for MR. Equilibrium time on the adsorption process occurred at 90 minutes with adsorption kinetics followed by pseudo-second-order (PSO). The adsorption isotherm followed the Langmuir isotherm equation. Data of thermodynamic parameters indicate that the adsorption process in this study occurs spontaneously and endothermically. The regeneration results show that Mg/Cr-Cu and Mg/Al-Cu can be used for the 5 cycles regeneration process of MO and MR adsorption process. Interactions that occur between adsorbents and adsorbate include physical interactions, interactions with the involvement of hydrogen bonds, and electrostatic interactions.

Keywords

modified LDH, metal oxide, adsorption, methyl orange, methyl red, regeneration

1 Introduction

The industrial sector is the fastest-growing development sector in Indonesia. Developments in this sector will, of course be followed by an increase in environmental pollution caused by waste, especially pollution in the aquatic environment, because in general industrial liquid waste is discharged directly into ditches or rivers. Industrial liquid waste is waste generated from various production processes in the industry. This liquid waste contains pollutants that cause the water to become colored [1–3].

The dyes in the textile industry that are widely used are methyl red and methyl orange which are types of anionic dyes [4]. The presence of dyes as waste is very disturbing to aesthetics and the environment. Water pollution due to dye waste will have a negative impact on the ecosystem and the surrounding environment, but this impact will be

visible in the long term. Therefore, it is necessary to treat the dye waste [5].

One way of processing dye waste that is quite optimal is using the adsorption method [6–9]. The process of handling liquid waste that has been contaminated with dyes through adsorption has many advantages, namely easy [10], simple [11], inexpensive [12], and effective [13]. The selection of the type of adsorbent in addition to being viewed from the side of effectiveness and selectivity in adsorption is also expected to be cheap and easy to manufacture. Layered double hydroxide (LDH) can be used as an alternative to a dye waste treatment [14].

Recently, LDHs have gained great attention from scientific researchers. LDHs have been used in various fields such as biomedicine, energy storage, photochemistry,

environment, etc. LDHs have advantages including low cost, high surface area, and high adsorption capacity [15, 16]. In improving the performance of LDH materials, it is necessary to modify the material so as to improve its physical performance and application. Materials that can be modified in LDH are metal oxides.

Research conducted by Taher et al. [17], a composite material based on montmorillonite–mixed metal oxides derived from ZnAl-LDH resulted in an adsorption capacity of 40 mg/g on the Congo Red dyes adsorption. Kumar et al. [18] said that ZnO and SnO₂ can remove malachite green oxalate dye with a maximum adsorption capacity of 310.50 mg/g and 216.90 mg/g. Research conducted by Budiman and Zuas [19] said that cerium dioxide nanoparticles (CeO₂-NP) can be used as an adsorbent to remove Acid Orange-10 dye with a maximum adsorption capacity of 33.33 mg/g. Nickel (II) oxide can be used as an adsorbent in the adsorption process of acid orange 7 (AO7) and indigo disulfonate (ID) with a maximum adsorption capacity of 178.57 mg/g and 227.27 mg/g [20].

In this study, modification of LDH materials, namely Mg/Al-LDH and Mg/Cr-LDH with metal oxide (Cu), was applied to the removal of anionic dyes including methyl orange (MO) and methyl red (MR). The use of two types of LDH material aims to see which modified material produces better performance on dye adsorption. The manufacture of metal oxides Mg/Al-Cu and Mg/Cr-Cu was carried out with the aim of increasing adsorption capacity; besides that, it was also expected that the interaction of functional groups on Mg/Al-Cu and Mg/Cr-Cu would have good stability. This research is expected to provide benefits for the handling of dye waste, thus environmental pollution can be handled as well as possible. The adsorption characteristics of MO and MR by adsorbents in terms of adsorption kinetics, adsorption isotherms, and adsorption thermodynamics, as well as the stability of the adsorbent structure were studied through regeneration studies.

2 Materials and methods

2.1 Materials

The materials used in this study such as Mg(NO₃)₂·6H₂O, Al(NO₃)₃·9H₂O, Cr(NO₃)₃·9H₂O, metal oxide used Cu(NO₃)₂·6H₂O, HCl, NaOH, distilled water, anionic dyes (MO and MR). The synthesized material was characterized using an X-Ray Rigaku Miniflex-600 diffractometer, Shimadzu Prestige-21 FTIR Spectrophotometer, BET Surface Area Analyzer Micrometric ASAP Quantachrome, and UV-Visible Biobase Spectrophotometer BKUV1800PC.

2.2 Methods

2.2.1 Synthesis of Mg/Cr and Mg/Al LDH

Synthesis of Mg/Cr LDH and Mg/Al-LDH was conducted as a similar procedure by Badri et al. [5] Mg/Cr and Mg/Al LDH were prepared in the following procedure: 100 mL of Mg(NO₃)₂·6H₂O 0.75 M solution and 100 mL of 0.25 M Al(NO₃)₃·9H₂O or Cr(NO₃)₃·9H₂O were mixed for 30 minutes, solution added NaOH 2 M solution until pH 10 and stirred for 24 hours at 353 K. The precipitate was filtered and dried at 383 K for 24 hours.

2.2.2 Synthesis Mg/Cr and Mg/Al LDH intercalated metal oxide

Mg/Cr and Mg/Al LDH intercalated metal oxide (Mg/Al-Cu and Mg/Cr-Cu) were prepared in the following procedure: as much as 100 mL of Mg(NO₃)₂·6H₂O 0.75 M and 100 mL of 0.25 M Al(NO₃)₃·9H₂O or Cr(NO₃)₃·9H₂O, and then added NaOH 2 M to pH 10 and stirred for 24 hours at 353 K. The mixture was added to 0.25 mL Cu(NO₃)₂·6H₂O 0.5 M. Precipitate was dried at 353 K for 24 hours, and then the process of calcination at a temperature of 523 K for 6 hours.

2.2.3 Adsorption studies

The effect of contact time on anionic dyes can be studied by varying the contact time (0, 10, 20, 30, 40, 50, 60, 70, 80, 90, 100, 120, and 150 minutes). 0.025 g adsorbent was added to a 50 mL Erlenmeyer containing 25 mL of dye solution with a concentration of 100 mg/L. The mixture was stirred, and the filtrate was measured using a UV-Visible spectrophotometer. The effect of concentration and temperature of adsorption was studied by varying the concentration (60, 70, 80, 90, and 100 mg/L) and temperature (303, 313, 323, and 333 K). 0.02 g adsorbent was added to an Erlenmeyer 50 mL containing 20 mL of MO and MR, stirring for 1 hour, and then the filtrate was measured using a UV-Visible spectrophotometer.

2.2.4 Regeneration process

Regeneration of adsorbent is carried out by adsorption and desorption processes first. MO and MR 100 mg/L were added with 0.1 g of adsorbent. The mixture was stirred for 2 hours, and the absorbance of the filtrate was measured using a UV-Visible spectrophotometer. Adsorbents that have been used are carried out the desorption process using the water-assisted ultrasonic system, then dried, and carried out for the next regeneration cycle by the same method.

3 Result and discussion

Materials of Mg/Cr-layered double hydroxide (Mg/Cr-LDH) and Mg/Al-layered double hydroxide (Mg/Al-LDH) intercalated metal oxide (Mg/Cr-Cu and Mg/Al-Cu) characterized using the X-ray diffraction (XRD), Fourier-transform infrared spectroscopy (FTIR), and Brunauer Emmett Teller (BET) analysis. The result of the XRD analysis is shown in Fig. 1. According to Badri et al. [21] diffraction pattern of Mg/Cr-LDH at angles 11° (003), 22° (006), 36° (115), and 60° (110). Fig. 1 (a) is a diffractogram pattern Mg/Cr-LDH shown characteristic of layered double hydroxide materials where diffraction peaks at angles of 12.45° and 61.44°. Based on data from the JCPDS File No. 20-0658, the diffractogram of Mg/Al-LDH is around angles 11.8° (003), 23.6° (006), 62.3° (113), and 66.3° (116) [22]. Fig. 1 (c) is a diffractogram of Mg/Al-LDH, which shows the peaks at 11.47°, 22.86°, 61.62°, and 65.5°, which indicates that the Mg/Al LDH synthesis process has been successfully carried out. The XRD results of Mg/Cr-Cu and Mg/Al-Cu powder shown in Fig. 1 (b) and (d) indicated the material is a metal oxide where diffraction pattern at angles of 31.73°, 33°, and 45.44°.

Based on the diffraction peaks of Mg/Cr-Cu and Mg/Al-Cu, the material has decreased crystallinity caused by the calcination process. Calcination of samples at 773 K or fewer leads to the collapse of the lamellar structure and new diffraction lines originating from metal oxides that exhibit lower crystallinity. Calcination at higher temperatures (>773 K) will result in increased crystallinity of the metal oxide [23, 24]. In this study, the calcination process

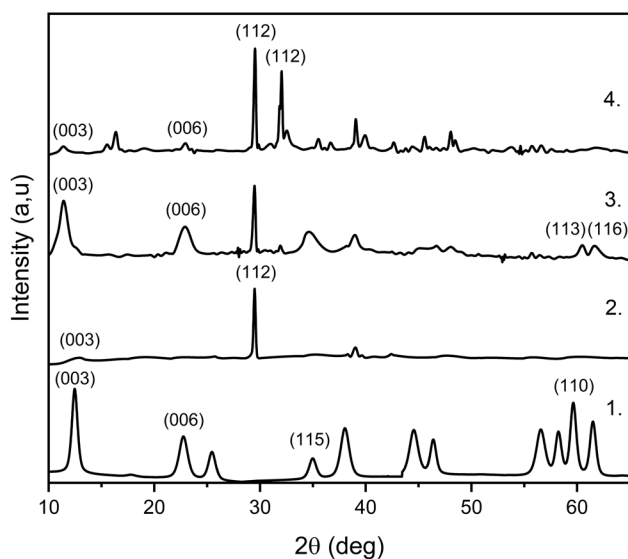


Fig. 1 XRD analysis of 1. Mg/Cr-LDH, 2. Mg/Cr-Cu, 3. Mg/Al-LDH, and 4. Mg/Al-Cu

was carried out at 523 K. This aims to produce metal oxide (Cu) without eliminating the material characteristics of LDH in the composite material.

The results of the FT-IR characterization of materials are shown in Fig. 2. FT-IR spectra of all materials have similar spectra showing stretch vibration of the O-H group indicated at 3471 cm⁻¹ and 3448 cm⁻¹. The spectrum at wavenumbers 1635 cm⁻¹ is O-H bending. Carbonate bands appeared at 1381 cm⁻¹ and 1331 cm⁻¹. Metallic oxygen bonding at 455 cm⁻¹ and 833 cm⁻¹. Characteristics for vibrations lower than 800 cm⁻¹ indicated the metallic oxygen bonding (M-O).

The graphs of nitrogen adsorption-desorption isotherms of materials shown in Fig. 3 indicate that the material has hysteresis and follows type IV isotherms. According to Ahmad et al. [25], type IV isotherm shows hysteresis of mesoporous-sized materials with strong hysteresis activity on the adsorbent-adsorbate interaction. Based on data BET analysis in Table 1, Mg/Cr-LDH and Mg/Al-LDH modified with metal oxide (Mg/Cr-Cu and Mg/Al-Cu) through the co-precipitation method showed increased surface area. Mg/Cr-LDH intercalated metal oxide increased its surface area from 21.5 to 38.9 m²/g, while the surface area of Mg/Al-LDH from 23.1 to 30.5 m²/g. The surface area of Mg/Cr-Cu is larger than the others because the material produces a smaller pore size and pore volume, so the formation of more functional groups is produced. More functional groups will affect the surface area of the material. Formation of a smaller surface area, it is caused by the agglomeration process (increase in particle size) in the material. The pore sizes of the materials were

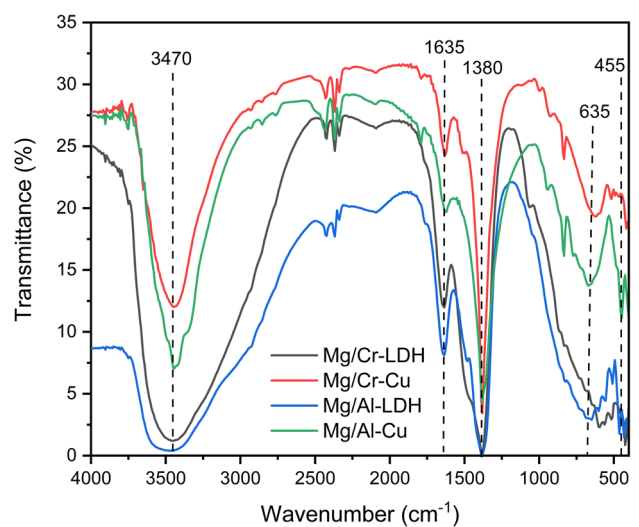


Fig. 2 FT-IR Spectra of Mg/Cr-LDH, Mg/Cr-Cu Mg/Al-LDH, and Mg/Al-Cu

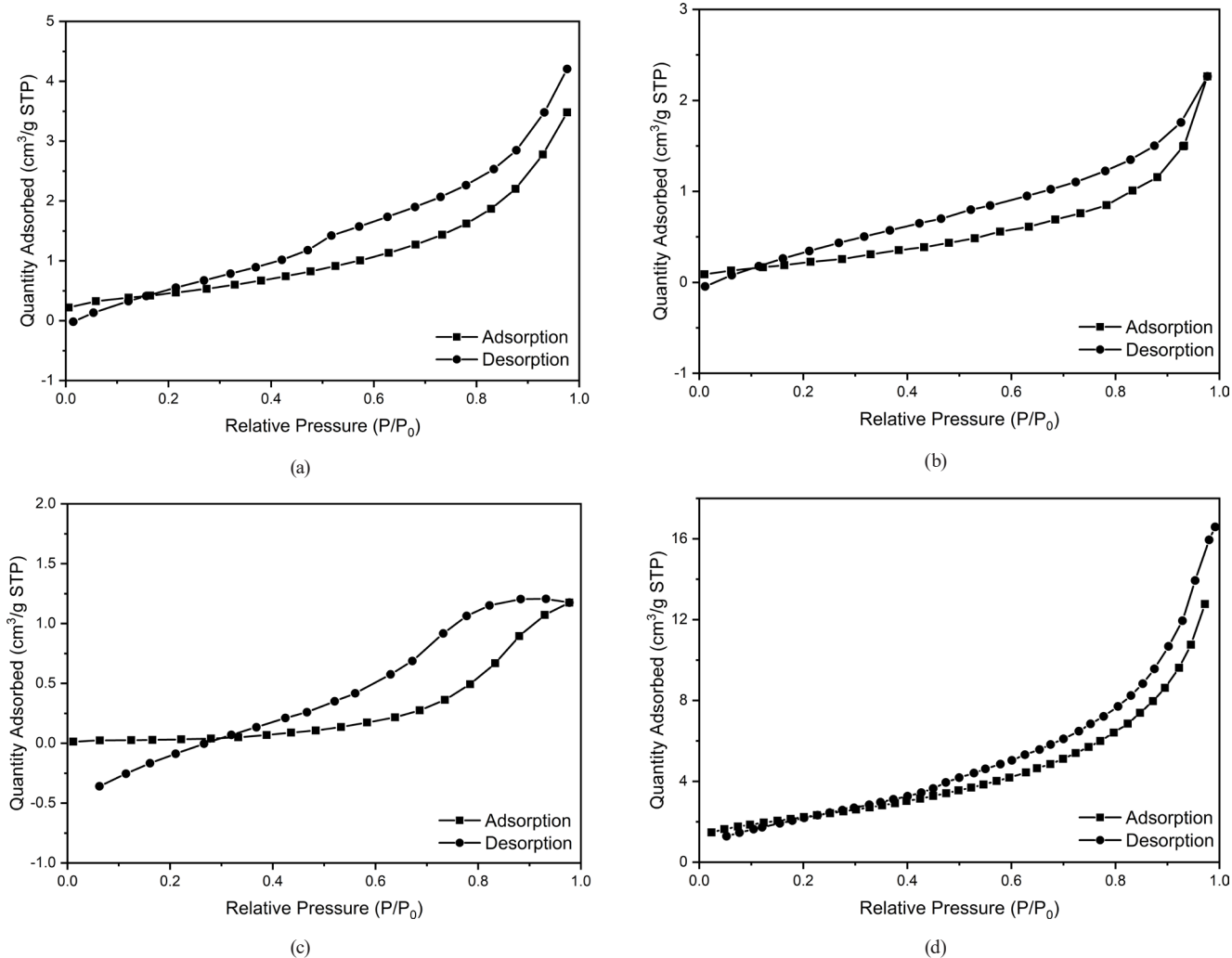


Fig. 3 BET profile of Mg/Cr-LDH (a), Mg/Cr-Cu (b), Mg/Al-LDH (c), and Mg/Al-Cu (d)

Table 1 Results of BET analysis

Adsorbent	Surface area (m ² /g)	Pore size (nm), Barrett Joyner Halenda (BJH)	Pore rolume (cm ³ /g), BJH
Mg/Cr-LDH	21.5	3.2	6.6
Mg/Al-LDH	23.2	0.09	3.6
Mg/Cr-Cu	38.9	0.09	3.2
Mg/Al-Cu	30.5	0.05	4.01

0.05–3.2 nm confirming that the mesoporous structure (range 2–50 nm) [25], and pore volume of the materials were 3.2–6.6 cm³/g. Mg/Cr-LDH has a larger pore diameter and pore volume.

Materials are applied as adsorbents in the MO and MR adsorption process, with varying contact times and the initial concentration of dyes on adsorption temperature, desorption process, and regeneration process. Based on the results of the adsorption contact time shown in Fig. 4, the equilibrium adsorption of MO and MR occurred at 90 minutes, with an insignificant increase in adsorption concentration at a contact time of more than 90 minutes.

Based on data Table 2 shows that the adsorption kinetics followed pseudo-second-order (PSO), with the value of the linear regression coefficient (R^2), which is close to the value 1 [12]. It revealed that the adsorption process indicates the involvement of chemisorption between adsorbent and adsorbate [26]. The kinetic model of PSO also shows that the process occurs influenced by adsorbents and adsorbates [27]. PFO and PSO equations are described in Eqs. (1) and (2) respectively:

$$\log(Q_e - Q_t) = \log Q_e - \left(\frac{k_1}{2.303} \right) t, \quad (1)$$

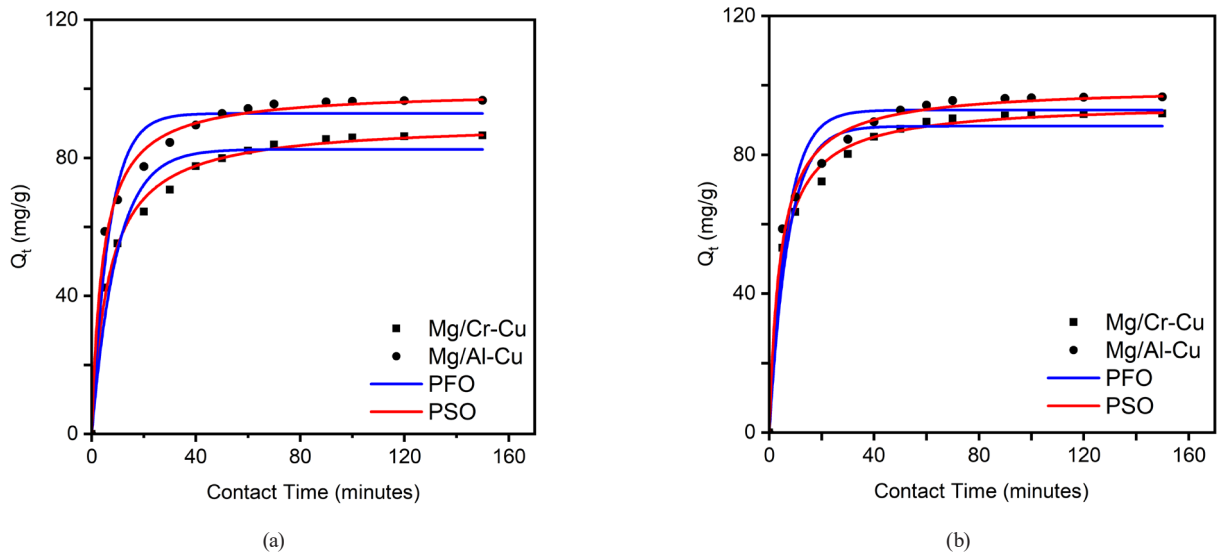


Fig. 4 Adsorption time contact of MO (a) and MR (b)

Table 2 Kinetic parameter

Adsorbent	Adsorbate	C_0 (mg/L)	$Q_{e_{exp}}$ (mg/g)	$Q_{e_{calc}}$ (mg/g)	PFO		PSO		
					R^2	k_1 (min ⁻¹)	$Q_{e_{calc}}$ (mg/g)	R^2	k_2 (g/mg min)
Mg/Cr-Cu	MO	106.3	86.5	60.6	0.993	0.05	91.7	0.999	0.001
Mg/Al-Cu			95.5	78.4	0.997	0.06	102.04	0.998	0.001
Mg/Al-Cu	MR	106.3	91.9	55.7	0.999	0.06	95.2	0.999	0.002
Mg/Cr-Cu			96.6	63.5	0.994	0.06	100	0.999	0.002

$$\frac{t}{Q_t} = \frac{1}{k_2 Q_e^2} + \frac{1}{Q_e} t, \quad (2)$$

where Q_e is the adsorption capacity at equilibrium (mg/g), Q_t is the adsorption capacity at time t (mg/g), t is contact time (min), k_1 is equilibrium rate constant for the PFO model (min⁻¹), and k_2 is equilibrium rate constant for the PSO model (g/mg min).

Based on data of effect the initial concentration of MO and MR in Figs. 5 and 6 indicates that increasing temperature causes an increase in concentration adsorption. Table 3 shows the large adsorption capacity that occurred at an adsorption temperature of 333 K. The adsorption capacity of Mg/Cr-Cu is 64.5 mg/g for MO and 78.8 for MR, and the adsorption capacity of Mg/Al-Cu is

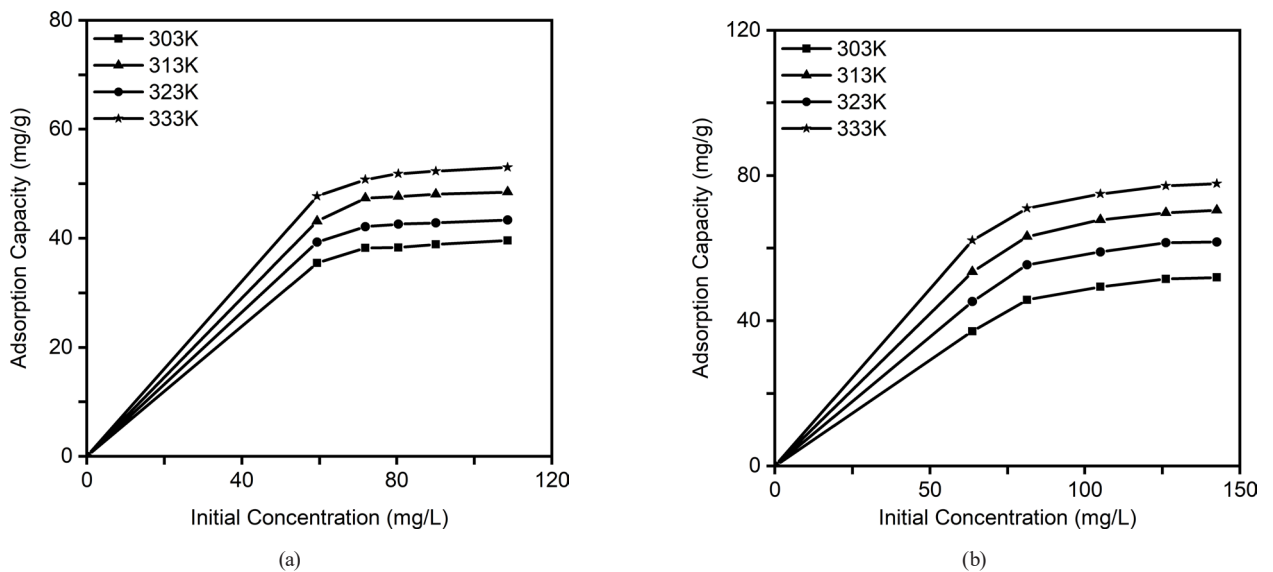


Fig. 5 Effect of initial concentration of MO (a) and MR (b) on adsorption temperature using Mg/Cr-Cu

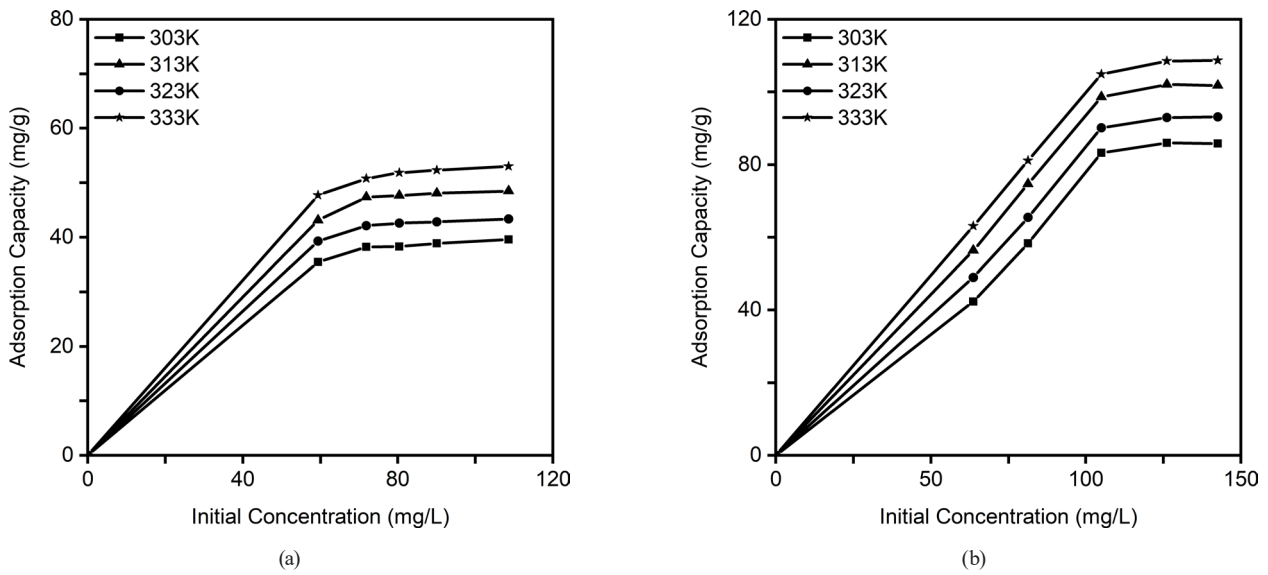


Fig. 6 Effect of initial concentration of MO (a) and MR (b) on adsorption temperature using Mg/Al-Cu

Table 3 Isotherm adsorption

Adsorbent	Adsorbate	Adsorption isotherm	Adsorption constant	T (K)			
				303 K	313 K	323 K	333 K
Mg/Cr-Cu	MO	Langmuir	Q_{max}	50	53.8	59.9	64.5
			k_L	0.06	0.08	0.1	0.1
			R^2	0.978	0.988	0.992	0.997
		Freundlich	n	0.99	0.99	0.99	0.99
			k_F	1.4	1.4	1.4	1.4
			R^2	0.979	0.973	0.991	0.995
Mg/Al-Cu	MO	Langmuir	Q_{max}	83.3	94.3	94.3	97.1
			k_L	0.1	0.1	0.2	0.7
			R^2	0.986	0.972	0.993	0.998
		Freundlich	n	0.91	0.98	0.98	0.99
			k_F	1.1	1.4	1.5	1.5
			R^2	0.977	0.897	0.962	0.995
Mg/Cr-Cu	MR	Langmuir	Q_{max}	61	68.02	74.1	78.8
			k_L	0.1	0.1	0.3	1.1
			R^2	0.993	0.997	0.999	0.999
		Freundlich	n	0.98	0.99	0.99	0.99
			k_F	1.4	1.4	1.5	1.5
			R^2	0.997	0.998	0.993	0.993
Mg/Al-Cu	MR	Langmuir	Q_{max}	104.2	105.2	106.3	108.7
			k_L	0.1	0.1	0.7	3
			R^2	0.902	0.966	0.996	0.999
		Freundlich	n	0.99	0.99	0.99	0.99
			k_F	1.5	1.6	1.6	1.6
			R^2	0.838	0.918	0.877	0.994

97.1 mg/g for MO and 108.7 mg/g for MR. The adsorption isotherm is shown in Table 3. The Langmuir model is better than the Freundlich model in the adsorption process

in this study, with the value of R^2 closer to the value of 1 [28, 29]. Langmuir and Freundlich isotherm equations are described in Eqs. (3) and (4) respectively:

$$\frac{C_e}{Q_e} = \frac{C_e}{Q_m} + \frac{1}{Q_m k_L} \quad (3)$$

$$\log Q_e = \log k_F + 1/n \log C_e \quad (4)$$

where C_e is the concentration of the dye solution at the equilibrium (mg/L), Q_e is the adsorption capacity at the equilibrium (mg/g), Q_m is the maximum adsorption capacity (mg/g), $1/n$ is the empirical parameter associated with surface heterogeneity, k_L is the adsorption constant of the Langmuir model (L/g), and k_F is the adsorption constant of the Freundlich model (mg/g (L/g)^{-1/n}). In general, the Langmuir isotherm model assumes that a monolayer adsorption process can occur on the adsorbent surface without mutual interaction between adsorbed molecules (chemisorption), while the Freundlich isotherm model involves not only adsorption on adsorbents with inhomogeneous surfaces but also adsorption between adsorbed molecules, or the adsorption process occurs in a multilayer (physisorption) [30, 31]. This study tends to follow the Langmuir isotherm model, which assumes the adsorption process occurs in a monolayer manner (chemisorption).

The thermodynamic parameters of materials are shown in Tables 4–7. A positive ΔH value indicates that

Table 4 Thermodynamic adsorption of MO using Mg/Cr-Cu

Concentration (mg/L)	T (K)	Q _e (mg/g)	ΔH (kJ/mol)	ΔS (J/mol K)	ΔG (kJ/mol)
63.1	303	29.6	26.5	0.09	0.4
	313	32.9			-0.4
	323	38.8			-1.3
	333	43.7			-2.1
83.9	303	38.6	20.6	0.07	0.4
	313	43.2			-0.2
	323	49.1			-0.9
	333	53.5			-1.6
102.6	303	40.5	17.6	0.05	1.1
	313	45.3			0.6
	323	51.3			0.01
	333	56.3			-0.5
122.1	303	41.5	16	0.05	1.7
	313	46.2			1.2
	323	52.7			0.8
	333	57.9			0.3
142.9	303	41.7	15	0.04	2.3
	313	46.6			1.8
	323	53			1.4
	333	58.7			1.01

Table 5 Thermodynamic adsorption of MR using Mg/Cr-Cu

Concentration (mg/L)	T (K)	Q _e (mg/g)	ΔH (kJ/mol)	ΔS (J/mol K)	ΔG (kJ/mol)
63.7	303	37.1	89.8	0.3	0
	313	45.3			-3
	323	53.4			-5.9
	333	62.2			-8.9
81.3	303	45.7	46.1	0.2	-0.5
	313	55.4			-2.1
	323	63.2			-3.6
	333	71			-5.1
105.1	303	49.4	28.9	0.1	0.3
	313	58.9			-0.6
	323	67.8			-1.6
	333	74.9			-2.5
126.1	303	51.5	23	0.1	0.9
	313	61.5			0.2
	323	69.7			-0.6
	333	77.2			-1.3
142.5	303	51.9	20.7	0.1	1.4
	313	61.6			0.7
	323	70.4			0.1
	333	77.8			-0.5

Table 6 Thermodynamic Adsorption of MO Using Mg/Al-Cu

Concentration (mg/L)	T (K)	Q _e (mg/g)	ΔH (kJ/mol)	ΔS (J/mol K)	ΔG (kJ/mol)
63.1	303	40.2	52.2	0.2	-1.2
	313	46.3			-2.9
	323	52.8			-4.7
	333	58			-6.4
83.9	303	54.7	53.9	0.2	-1.3
	313	62.4			-3.1
	323	70.3			-4.9
	333	78			-6.7
102.6	303	65.6	30.7	0.1	-1.3
	313	72.3			-2.4
	323	79.1			-3.4
	333	86.5			-4.5
122.1	303	68.5	23.1	0.1	-0.6
	313	76.2			-1.4
	323	83.4			-2.1
	333	91.1			-2.9
142.9	303	70.3	17.8	0.1	0.1
	313	77			-0.5
	323	84.7			-1
	333	92.3			-1.6

Table 7 Thermodynamic Adsorption of MR Using Mg/Al-Cu

Concentration (mg/L)	T (K)	Q_e (mg/g)	ΔH (kJ/mol)	ΔS (J/mol K)	ΔG (kJ/mol)
63.7	303	42.3	54.8	0.2	-1.6
	313	49			-3.4
	323	56.3			-5.3
	333	63.1			-7.1
81.3	303	58.4	59.8	0.2	-2.1
	313	65.5			-4.2
	323	74.6			-6.2
	333	81.1			-8.3
105.1	303	83.3	56.4	0.2	-3.2
	313	90.1			-5.1
	323	98.7			-7.1
	333	104.9			-9.1
126.1	303	85.9	30	0.1	-1.8
	313	93			-2.9
	323	102.1			-3.9
	333	108.5			-5
142.5	303	85.8	21.2	0.1	-1
	313	93.1			-1.7
	323	101.8			-2.5
	333	108.7			-3.2

the adsorption is an endothermic process [32, 33], while a ΔS value indicates that the degree of irregularity in the adsorption process is small in large concentrations, and the overall ΔG value is negative, indicating a spontaneous adsorption process [34, 35]. The thermodynamic parameters were calculated by Eqs. (5) and (6):

$$\ln \frac{Q_e}{C_e} = \frac{\Delta S}{R} - \frac{\Delta H}{RT}, \quad (5)$$

$$\Delta G = \Delta H - T\Delta S, \quad (6)$$

where T is the temperature (K), R is the molar gas constant (8.314), ΔH is the enthalpy (kJ/mol), ΔS is the entropy (J mol/K), and ΔG is Gibbs free energy (kJ/mol).

Table 8 shows the maximum adsorption capacity of methyl orange and methyl red using various types of adsorbents. Table 8 confirms that the maximum adsorption capacity of MO and MR using Mg/Cr-Cu and Mg/Al-Cu adsorbents in this study is greater than the adsorbents shown in Table 8 [36–47].

Based on data of the regeneration process in Fig. 7, materials of Mg/Cr-Cu and Mg/Al-Cu can be used in the five cycles regeneration process of MO and MR adsorption process. In the last cycle, the percentage adsorption of MO using Mg/Cr-Cu and Mg/Al-Cu is about 30%, while in MR about 40% for Mg/Cr-Cu and 80% for Mg/Al-Cu. This indicates that the Mg/Cr-LDH and Mg/Al-LDH after intercalated metal oxide (Cu) improved performance in process regeneration. The MR adsorption process produces a greater adsorption capacity than MO, it can occur assumed due to the difference in molecular weight (MO > MR) and the chemical interactions that occur. It also affects the results of adsorbent regeneration, where the regeneration process has better efficiency for MR removal compared to MO when using Mg-Cr/Cu and Mg-Al/Cu.

Table 8 Comparison of adsorption capacity on MO and MR adsorption by several adsorbents

Adsorbent	Adsorbate	Adsorption capacity (mg/g)	Reference
Functionalized CNTs/TiO ₂	MO	42.68	[36]
Fe ₂ O ₃ /mesoporous carbon		35.12	[37]
Bi ₂ O ₃ /TiO ₂ /powdered AC		16.33	[38]
Chitosan/diatom		35.12	[39]
NaX/MgO-TiO ₂ zeolite		53.76	[40]
LDH/Fe ₃ O ₄ /polyvinyl		19.59	[41]
Mg/Cr-Cu		64.5	This research
Mg/Al-Cu		97.1	This research
Activated carbon	MR	40.48	[42]
Coal Fly Ash		22.22	[43]
Eggshell		1.66	[44]
<i>Nephelium lappaceum</i>		62.66	[45]
Granular Activated Carbon		1.17	[46]
Lemon grass		72.32	[47]
Mg/Cr-Cu		78.7	This research
Mg/Al-Cu		108.7	This research

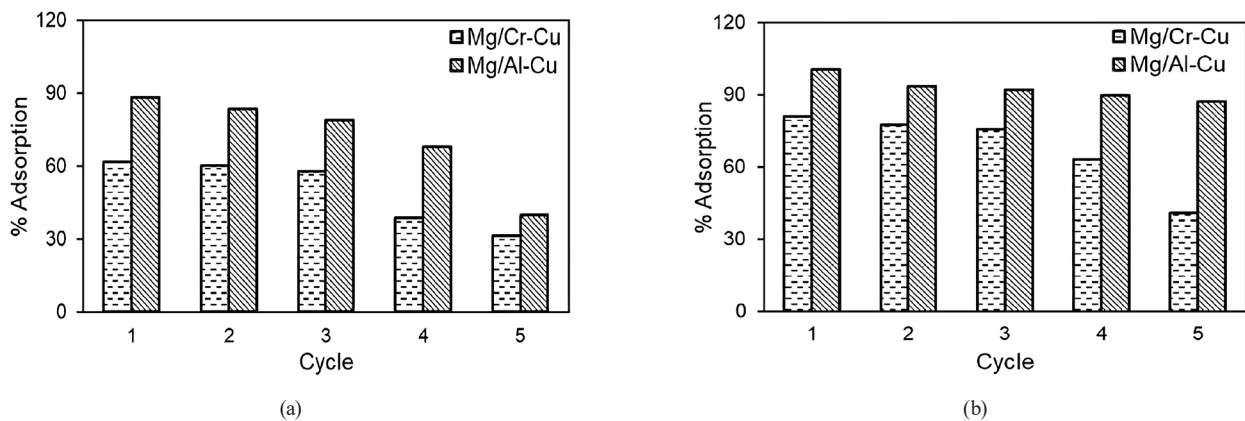


Fig. 7 Regeneration of materials on MO (a) and MR (b)

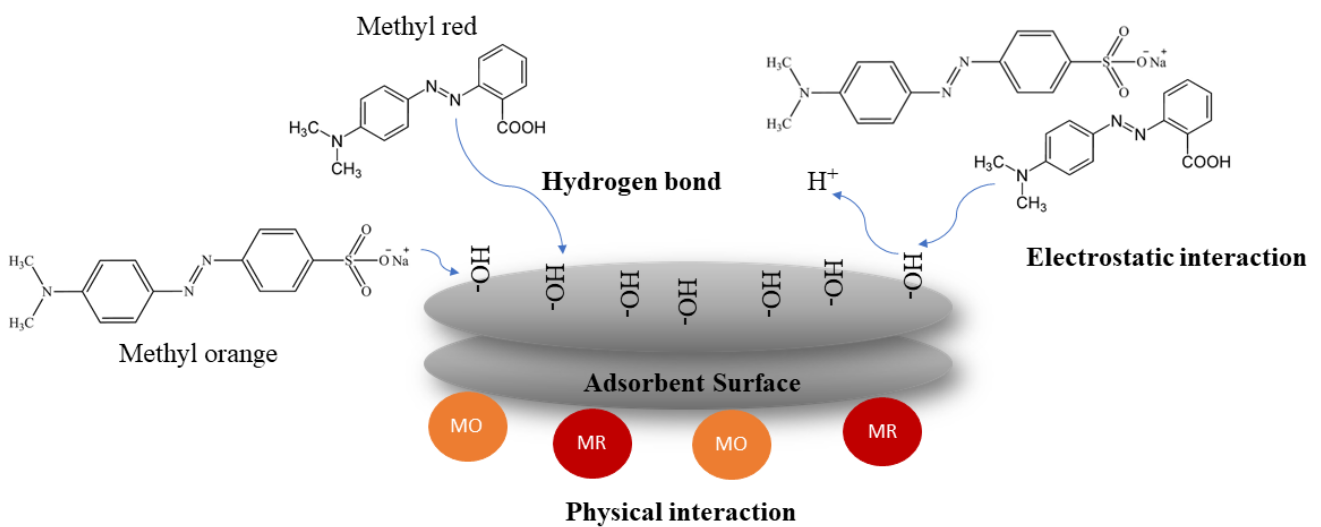


Fig. 8 Schematic illustration of MO and MR adsorption mechanism onto Mg/Cr-Cu and Mg/Al-Cu

A schematic illustration of the MO and MR adsorption mechanism using Mg/Cr-Cu and Mg/Al-Cu is presented in Fig. 8, the possible interactions that occur between adsorbents and adsorbate include physical interactions, interactions with the involvement of hydrogen bonds, and electrostatic interactions.

4 Conclusion

Mg/Cr-LDH intercalated metal oxide increased its surface area from 21.5 to 38.9 m²/g, while the surface area of Mg/Al-LDH from 23.2 to 30.5 m²/g. Based on data obtained from this study, it can be concluded that the largest adsorption capacity occurred at a temperature of 333 K, where the adsorption capacity of Mg/Cr-Cu is 64.5 mg/g for MO

and 78.8 mg/g for MR, and the adsorption capacity of Mg/Al-Cu is 97.1 mg/g for MO and 108.7 mg/g for MR. The adsorption kinetics followed PSO for MO and MR. The adsorption isotherm followed the Langmuir isotherm with a value of *R*² closer to the value of 1. Adsorption in this study includes an endothermic process and occurs spontaneously. Based on data, the regeneration results show that Mg/Cr-Cu and Mg/Al-Cu can be used for 5 cycles regeneration process of MO and MR adsorption process.

Acknowledgment

The authors thank to Research Centre of Inorganic Materials and Coordination Complexes FMIPA Sriwijaya University for supporting instrumental analysis.

References

- [1] Zenasni, M. A., Meroufel, B., Merlin, A., George, B. "Adsorption of Congo Red from Aqueous Solution Using CTAB-Kaolin from Bechar Algeria", *Journal of Surface Engineered Materials and Advanced Technology*, 4(6), pp. 332–341, 2014.
<https://doi.org/10.4236/jsemat.2014.46037>
- [2] Attallah, M. F., Ahmed, I. M., Hamed, M. M. "Treatment of industrial wastewater containing Congo Red and Naphthol Green B using low-cost adsorbent", *Environmental Science and Pollution Research*, 20(2), pp. 1106–1116, 2013.
<https://doi.org/10.1007/s11356-012-0947-4>
- [3] Mallakpour, S., Azadi, E., Dinari, M. "Removal of cationic and anionic dyes using Ca-alginate and Zn-Al layered double hydroxide/metal-organic framework", *Carbohydrate Polymers*, 301, 120362, 2023.
<https://doi.org/10.1016/j.carbpol.2022.120362>
- [4] Tao, X., Han, Y., Sun, C., Huang, L., Xu, D. "Plasma modification of NiAlCe–LDH as improved photocatalyst for organic dye wastewater degradation", *Applied Clay Science*, 172, pp. 75–79, 2019.
<https://doi.org/10.1016/j.clay.2019.02.020>
- [5] Badri, A. F., Juleanti, N., Palapa, N. R., Hanifah, Y., Mohadi, R., Mardiyanto, M., Lesbani, A. "Oxalate intercalated Mg/Cr layered double hydroxide as adsorbent of methyl red and methyl orange from aqueous solution", *Ecological Engineering & Environmental Technology*, 22(3), pp. 71–81, 2021.
<https://doi.org/10.12912/27197050/135509>
- [6] Lyu, P., Wang, G., Wang, B., Yin, Q., Li, Y., Deng, N. "Adsorption and interaction mechanism of uranium (VI) from aqueous solutions on phosphate-impregnation biochar cross-linked Mg–Al layered double-hydroxide composite", *Applied Clay Science*, 209, 106146, 2021.
<https://doi.org/10.1016/j.clay.2021.106146>
- [7] Azha, S. F., Hamid, S. A., Ismail, S. "Development of composite adsorbent coating based acrylic polymer/bentonite for methylene blue removal", *Journal of Engineering and Technological Sciences*, 49(2), pp. 225–235, 2017.
<https://doi.org/10.5614/j.eng.technol.sci.2017.49.2.5>
- [8] Zubair, M., Jarrah, N., Ihsanullah, Khalid, A., Manzar, M. S., Kazeem, T. S., Al-Harthi, M. A. "Starch-NiFe-layered double hydroxide composites: Efficient removal of methyl orange from aqueous phase", *Journal of Molecular Liquids*, 249, pp. 254–264, 2018.
<https://doi.org/10.1016/j.molliq.2017.11.022>
- [9] Vishal, K., Aruchamy, K., Sriram, G., Ching, Y. C., Oh, T. H., Hegde, G., Ajeya, K. V., Joshi, S., Sowrirrajan, A. V., Jung, H.-Y., Kurkuri, M. "Engineering a low-cost diatomite with Zn-Mg-Al Layered triple hydroxide (LTH) adsorbents for the effectual removal of Congo red: Studies on batch adsorption, mechanism, high selectivity, and desorption", *Colloids and Surfaces A: Physicochemical and Engineering Aspects*, 661, 130922, 2023.
<https://doi.org/10.1016/j.colsurfa.2023.130922>
- [10] Lv, X., Qin, X., Wang, K., Peng, Y., Wang, P., Jiang, G. "Nanoscale zero valent iron supported on MgAl-LDH-decorated reduced graphene oxide: Enhanced performance in Cr(VI) removal, mechanism and regeneration", *Journal of Hazardous Materials*, 373, pp. 176–186, 2019.
<https://doi.org/10.1016/j.jhazmat.2019.03.091>
- [11] Tang, Z., Qiu, Z., Lu, S., Shi, X. "Functionalized layered double hydroxide applied to heavy metal ions absorption: A review", *Nanotechnology Reviews*, 9(1), pp. 800–819, 2020.
<https://doi.org/10.1515/ntrev-2020-0065>
- [12] Nwodika, C., Onukwuli, D. O. "Adsorption Study of Kinetics and Equilibrium of Basic Dye on Kola Nut Pod Carbon", *Gazi University Journal of Science*, 30(4), pp. 86–102, 2017. [online] Available at: <https://dergipark.org.tr/en/pub/gujs/issue/32802/315642> [Accessed: 15 November 2022]
- [13] Hu, H., Wageh, S., Al-Ghamdi, A. A., Yang, S., Tian, Z., Cheng, B., Ho, W. "NiFe-LDH nanosheet/carbon fiber nanocomposite with enhanced anionic dye adsorption performance", *Applied Surface Science*, 511, 145570, 2020.
<https://doi.org/10.1016/j.apsusc.2020.145570>
- [14] Lee, S. Y., Choi, J.-W., Song, K. G., Choi, K., Lee, Y. J., Jung, K. W. "Adsorption and mechanistic study for phosphate removal by rice husk-derived biochar functionalized with Mg/Al-calcined layered double hydroxides via co-pyrolysis", *Composites Part B: Engineering*, 176, 107209, 2019.
<https://doi.org/10.1016/j.compositesb.2019.107209>
- [15] Sriram, G., Bendre, A., Altalhi, T., Jung, H.-Y., Hegde, G., Kurkuri, M. "Surface engineering of silica based materials with Ni–Fe layered double hydroxide for the efficient removal of methyl orange: Isotherms, kinetics, mechanism and high selectivity studies", *Chemosphere*, 287, 131976, 2022.
<https://doi.org/10.1016/j.chemosphere.2021.131976>
- [16] Zhou, H., Wu, F., Fang, L., Hu, J., Luo, H., Guan, T., Hu, B., Zhou, M. "Layered NiFe-LDH/MXene nanocomposite electrode for high-performance supercapacitor", *International Journal of Hydrogen Energy*, 45(23), pp. 13080–13089, 2020.
<https://doi.org/10.1016/j.ijhydene.2020.03.001>
- [17] Taher, T., Munandar, A., Mawaddah, N., Wisnubroto, M. S., Siregar, P. M. S. B. N., Palapa, N. R., Lesbani, A., Wibowo, Y. G. "Synthesis and characterization of montmorillonite – Mixed metal oxide composite and its adsorption performance for anionic and cationic dyes removal", *Inorganic Chemistry Communications*, 147, 110231, 2023.
<https://doi.org/10.1016/j.inoche.2022.110231>
- [18] Kumar, K. Y., Muralidhara, H. B., Nayaka, Y. A., Balasubramanyam, J., Hanumanthappa, H. "Low-cost synthesis of metal oxide nanoparticles and their application in adsorption of commercial dye and heavy metal ion in aqueous solution", *Powder Technology*, 246, pp. 125–136, 2013.
<https://doi.org/10.1016/j.powtec.2013.05.017>
- [19] Budiman, H., Zuas, O. "Adsorption isotherm studies on acid orange-10 dye removal using cerium dioxide nanoparticles", *Indonesian Journal of Chemistry*, 14(3), pp. 226–232, 2014.
<https://doi.org/10.22146/ijc.21232>
- [20] Huo, X., Zhang, Y., Zhang, J., Zhou, P., Xie, R., Wei, C., Liu, Y., Wang, N. "Selective adsorption of anionic dyes from aqueous solution by nickel (II) oxide", *Journal of Water Supply: Research and Technology-AQUA*, 68(3), pp. 171–186, 2019.
<https://doi.org/10.2166/aqua.2019.115>
- [21] Badri, A. F., Mohadi, R., Mardiyanto, M., Lesbani, A. "Adsorptive capacity of malachite green onto Mg/M3+ (M3+=Al and Cr) LDHs", *Global Nest Journal*, 23(1), pp. 82–89, 2021.
<https://doi.org/10.30955/gnj.003443>

- [22] Juleanti, N., Palapa, N. R., Taher, T., Hidayati, N., Putri, B. I., Lesbani, A. "The capability of biochar-based CaAl and MgAl composite materials as adsorbent for removal Cr(VI) in aqueous solution", *Science & Technology Indonesia*, 6(3), pp. 196–203, 2021. <https://doi.org/10.26554/sti.2021.6.3.196-203>
- [23] Abderrazek, K., Najoua, F. S., Srasra, E. "Synthesis and characterization of [Zn–Al] LDH: Study of the effect of calcination on the photocatalytic activity", *Applied Clay Science*, 119, pp. 229–235, 2016. <https://doi.org/10.1016/j.clay.2015.10.014>
- [24] Carriazo, D., del Arco, M., García-López, E., Marci, G., Martín, C., Palmisano, L., Rives, V. "Zn,Al hydrotalcites calcined at different temperatures: Preparation, characterization and photocatalytic activity in gas–solid regime", *Journal of Molecular Catalysis A: Chemical*, 342–343, pp. 83–90, 2011. <https://doi.org/10.1016/j.molcata.2011.04.015>
- [25] Ahmad, N., Arsyad, F. S., Royani, I., Lesbani, A. "Charcoal activated as template Mg/Al layered double hydroxide for selective adsorption of direct yellow on anionic dyes", *Results in Chemistry*, 5, 100766, 2023. <https://doi.org/10.1016/j.rechem.2023.100766>
- [26] Shahinpour, A., Tanhaei, B., Ayati, A., Beiki, H., Sillanpää, M. "Binary dyes adsorption onto novel designed magnetic clay-bio-polymer hydrogel involves characterization and adsorption performance: Kinetic, equilibrium, thermodynamic, and adsorption mechanism", *Journal of Molecular Liquids*, 366, 120303, 2022. <https://doi.org/10.1016/j.molliq.2022.120303>
- [27] Feng, T., Xu, L. "Adsorption of Congo red from aqueous solution onto chitosan/rectorite composite", *Advanced Materials Research*, 690–693, pp. 438–441, 2013. <https://doi.org/10.4028/www.scientific.net/AMR.690-693.438>
- [28] Siregar, P. M. S. B. N., Normah, Juleanti, N., Wijaya, A., Palapa, N. R., Mohadi, R., Lesbani, A. "Mg/Al-CH, Ni/Al-CH, and Zn/Al-CH as adsorbents for Congo Red removal in aqueous solution", *Communications in Science and Technology*, 6(2), pp. 74–79, 2021. <https://doi.org/10.21924/est.6.2.2021.547>
- [29] Chopra, M., Drivjot, Amita "Adsorption of Dyes from Aqueous Solution Using Orange Peels: Kinetics and Equilibrium", *Journal of Advanced Laboratory Research in Biology*, 3(1), pp. 1–8, 2012. [online] Available at: <http://e-journal.sospublication.co.in/index.php/ab/article/view/67> [Accessed: 15 February 2022]
- [30] Lv, H.-W., Jiang, H.-J., He, F.-A., Hu, Q.-D., Zhong, Z.-R., Yang, Y.-Y. "Adsorption of anionic and cationic dyes by a novel cross-linked cellulose-tetrafluoroterephthalonitrile-tannin polymer", *European Polymer Journal*, 180, 111602, 2022. <https://doi.org/10.1016/j.eurpolymj.2022.111602>
- [31] Chen, X., Hossain, M. F., Duan, C., Lu, J., Tsang, Y. F., Islam, M. S., Zhou, Y. "Isotherm models for adsorption of heavy metals from water - A review", *Chemosphere*, 307, 135545, 2022. <https://doi.org/10.1016/j.chemosphere.2022.135545>
- [32] Iftekhar, S., Ramasamy, D. L., Srivastava, V., Asif, M. B., Sillanpää, M. "Understanding the factors affecting the adsorption of Lanthanum using different adsorbents: A critical review", *Chemosphere*, 204(4), pp. 413–430, 2018. <https://doi.org/10.1016/j.chemosphere.2018.04.053>
- [33] Yudha, S. P., Tekasakul, S., Phoungthong, K., Chuenchom, L. "Green synthesis of low-cost and eco-friendly adsorbent for dye and pharmaceutical adsorption: Kinetic, isotherm, thermodynamic and regeneration studies", *Materials Research Express*, 6(12), 125526, 2019. <https://doi.org/10.1088/2053-1591/ab58ae>
- [34] Patil, M. A., Shinde, J. K., Jadhav, A. L., Deshpande, S. R. "Adsorption of methylene blue in waste water by low cost adsorbent rice husk", [pdf] *International Journal of Engineering Research & Technology*, 10(1), pp. 246–252, 2017. Available at: https://www.ripublication.com/irph/ijert_spl17/ijertv10n1spl_47.pdf [Accessed: 18 January 2023]
- [35] Wang, P., Yan, T., Wang, L. "Removal of Congo red from aqueous solution using magnetic chitosan composite microparticles", *BioResources*, 8(4), pp. 6026–6043, 2013.
- [36] Ahmad, A., Razali, M. H., Mamat, M., Mehamod, F. S. B., Amin, K. A. M. "Adsorption of methyl orange by synthesized and functionalized-CNTs with 3-aminopropyltriethoxysilane loaded TiO₂ nanocomposites", *Chemosphere*, 168, pp. 474–482, 2017. <https://doi.org/10.1016/j.chemosphere.2016.11.028>
- [37] Xiao, Y., Hill, J. M. "Impact of pore size on Fenton oxidation of methyl orange adsorbed on magnetic carbon materials: Trade-off between capacity and regenerability", *Environmental Science & Technology*, 51(8), pp. 4567–4575, 2017. <https://doi.org/10.1021/acs.est.7b00089>
- [38] Shang, Y., Li, X., Yang, Y., Wang, N., Zhuang, X., Zhou, Z. "Optimized photocatalytic regeneration of adsorption-photocatalysis bifunctional composite saturated with Methyl Orange", *Journal of Environmental Sciences*, 94, pp. 40–51, 2020. <https://doi.org/10.1016/j.jes.2020.03.044>
- [39] Zhao, P., Zhang, R., Wang, J. "Adsorption of methyl orange from aqueous solution using chitosan/diatomite composite", *Water Science & Technology*, 75(7), pp. 1633–1642, 2017. <https://doi.org/10.2166/wst.2017.034>
- [40] Mirzaei, D., Zabardasti, A., Mansourpanah, Y., Sadeghi, M., Farhadi, S. "Efficacy of Novel NaX/MgO–TiO₂ Zeolite Nanocomposite for the Adsorption of Methyl Orange (MO) Dye: Isotherm, Kinetic and Thermodynamic Studies", *Journal of Inorganic and Organometallic Polymers and Materials*, 30(6), pp. 2067–2080, 2020. <https://doi.org/10.1007/s10904-019-01369-9>
- [41] Mallakpour, S., Hatami, M. "An effective, low-cost and recyclable bio-adsorbent having amino acid intercalated LDH@Fe₃O₄/PVA magnetic nanocomposites for removal of methyl orange from aqueous solution", *Applied Clay Science*, 174, pp. 127–137, 2019. <https://doi.org/10.1016/j.clay.2019.03.026>
- [42] Santhi, T., Manonmani, S., Smitha, T. "Removal of Methyl Red from Aqueous Solution by Activated Carbon Prepared from the *Annona squamosa* Seed by Adsorption", *Chemical Engineering Research Bulletin*, 14(1), pp. 11–18, 2010. <https://doi.org/10.3329/cerb.v14i1.3767>
- [43] Bekele, B. A., Balcha, M. A., Demelash, F. B. "Adsorption of Methyl Red on Coal Fly Ash from Aqueous Solution", *Chemistry and Materials Research*, 10(4), pp. 13–19, 2018. [online] Available at: <https://core.ac.uk/display/234667128> [Accessed: 15 November 2022]

- [44] Rajoriya, S., Saharan, V. K., Pundir, A. S., Nigam, M., Roy, K. "Adsorption of methyl red dye from aqueous solution onto egg-shell waste material: Kinetics, isotherms and thermodynamic studies", *Current Research in Green and Sustainable Chemistry*, 4, 100180, 2021.
<https://doi.org/10.1016/j.crgsc.2021.100180>
- [45] Zein, R., Astuti, A. W., Wahyuni, D., Furqani, F., Khoiriah, Munaf, E. "Removal of Methyl Red from Aqueous Solution by *Nepthelium lappaceum*", [pdf] *Research Journal of Pharmaceutical, Biological and Chemical Sciences*, 6(3), pp. 86–97, 2015. Available at: [https://www.rjpbcs.com/pdf/2015_6\(3\)/\[11\].pdf](https://www.rjpbcs.com/pdf/2015_6(3)/[11].pdf) [Accessed: 15 November 2022]
- [46] Itodo, A. U., Usman, A., Akinrinmade, G., Itodo, H. U., Ugboaja, V. C. "Performance Assessment of Received and Formulated Carbon Animalis: A Comparative Adsorption Isotherm Test", *Journal of Environmental Protection*, 3(3), pp. 288–295, 2012.
<https://doi.org/10.4236/jep.2012.33036>
- [47] Ahmad, M. A., Ahmed, N. B., Adegoke, K. A., Bello, O. S. "Sorption studies of methyl red dye removal using lemon grass (*Cymbopogon citratus*)", *Chemical Data Collections*, 22, 100249, 2019.
<https://doi.org/10.1016/j.cdc.2019.100249>